pharmaceutics

MDPI

Article

Harnessing nanomedicine to potentiate the chemo-immunotherapeutic effects of doxorubicin and alendronate co-encapsulated in pegylated liposomes

Alberto Gabizon[1,2,*], Hilary Shmeeda[1], Benjamin Draper[3], Ana Parente-Pereira[3], John Maher[3], Amaia Carrascal-Miniño[4], Rafael T. M. de Rosales[4], Ninh M. La-Beck[5]

[1] Nano-Oncology Research Center, Oncology Institute, Shaare Zedek Medical Center, Jerusalem 9103102, Israel
[2] Faculty of Medicine, The Hebrew University of Jerusalem, Jerusalem 9112102, Israel
[3] King's College London, School of Cancer and Pharmaceutical Sciences, Guy's Cancer Centre, Great Maze Pond, London SE1 9RT, UK
[4] King's College London, School of Biomedical Engineering & Imaging Sciences, St. Thomas' Hospital, London SE1 7EH, UK
[5] Department of Immunotherapeutics and Biotechnology, Jerry H. Hodge School of Pharmacy, Texas Tech University Health Sciences Center, Abilene, TX 79601, USA
* Correspondence: alberto.gabizon@gmail.com; agabizon@szmc.org.il

Abstract: Encapsulation of Doxorubicin (Dox), a potent cytotoxic agent and immunogenic cell death inducer in pegylated (Stealth) liposomes is well known to have major pharmacologic advantages over treatment with free Dox. Reformulation of alendronate (Ald), a potent amino-bisphosphonate, by encapsulation in pegylated liposomes results in significant immune modulatory effects through interaction with tumor-associated macrophages and activation of a subset of gamma-delta T lymphocytes. We present here recent findings of our research work with a formulation of Dox and Ald co-encapsulated in pegylated liposomes (PLAD) and discuss its pharmacological properties vis-à-vis free Dox and the current clinical formulation of pegylated liposomal Dox. PLAD is a robust formulation with high and reproducible remote loading of Dox, and high stability in plasma. Results of biodistribution studies, imaging with radionuclide-labeled liposomes, and therapeutic studies as single agent and in combination with immune checkpoint inhibitors or gamma-delta T lymphocytes suggest that PLAD is a unique product with distinct tumor microenvironmental interactions and distinct pharmacologic properties when compared to free Dox and the clinical formulation of pegylated liposomal Dox. These results underscore the potential added value of PLAD for chemo-immunotherapy of cancer and the relevance of the co-encapsulation approach in nanomedicine.

Keywords: liposome; Doxorubicin; alendronate; co-encapsulation; chemotherapy; immunotherapy

Citation: To be added by editorial staff during production.

Academic Editor: Firstname Lastname

Received: date
Revised: date
Accepted: date
Published: date

1. Introduction

Co-encapsulation of multiple drugs in the same nanocarrier is a unique tool of nanomedicine offering multiple pharmacologic advantages such as co-delivery in space and time of two or more agents maximizing their additive or synergistic effects in cancer therapy or other fields of medical therapy. Formulating nanoparticles containing co-encapsulated drugs is an attractive strategy for co-delivery of drugs with different mechanisms of action and non-overlapping toxicities (1). Dual or multi-drug liposomes have been initially proposed by the group of Tolcher and Mayer (2) whose approach is based on screening *in vitro* for drug ratios that result in synergistic cytotoxicity. The field of co-encapsulation or co-delivery of multiple drugs in nanoparticles has attracted increased attention in recent years, particularly in cancer applications (2-7). This approach includes examples

of combinations of two cytotoxic drugs (8), one of which may be a prodrug (9), or one cytotoxic drug and an immunomodulatory drug (10). The success of this approach in humans is exemplified by the FDA approval of CPX-351 (Vyxeos®), an optimized ratio of daunorubicin and cytarabine co-encapsulated in liposomes which significantly improved survival in acute myeloid leukemia patients (AML) when tested against the conventional treatment with the same drug combination in free form (11).

We have developed a pegylated liposome formulation with 2 active ingredients, alendronate (Ald) and doxorubicin (Dox), referred to as PLAD, that display very different mechanisms of action and have no overlapping toxicity (12). The choice of Dox is well supported by a plethora of preclinical and clinical data asserting its compatibility with liposome formulations and its clinical value as anticancer agent (13). The choice of Ald is based on the multifaceted properties of aminobisphosphonates including direct (reduced tumor cell invasion and proliferation) and indirect (reduced osteoclastic activity and angiogenesis) antitumor effects (14, 15) along with immunological effects (increased activity of gamma-delta T cells and suppression of tumor-enhancing macrophages when formulated in liposomes) (16, 17). The lipid backbone of this formulation is very similar to the clinically approved formulation of pegylated liposomal Dox (PLD), known commercially as Doxil/Caelyx® or LipoDox for the generic version. We have previously reported that PLAD significantly affects the composition profile and functionality of tumor-infiltrating immune cells (18). We report here on various improvements of the pharmaceutical technology and characterization of the PLAD (Pegylated Liposomal Ald-Dox) formulation (12), and explore further aspects of its biological performance *in vitro* and *in vivo*.

2. Materials and Methods

Chemicals sources:

Hydrogenated soybean phosphatidylcholine (HSPC), Lipoid GmbH, Ludwigshafen, Germany; methoxy-polyethylene glycol-distearoyl-phosphatidylethanolamine ($mPEG_{2000}$-DSPE); Bio-Lab Ltd., Jerusalem, Israel; cholesterol (Chol) and ammonium hydroxide (Sigma, St. Louis, MO, USA); Alendronic acid (Ald), Tokyo Chemical Industry Co Ltd., Japan; Doxorubicin HCl (Dox), Teva Pharmaceuticals, Tel Aviv, Israel; Pegylated liposomal doxorubicin (PLD), either as Doxil/Caelyx™ (Janssen Pharmaceuticals, Beerse, Belgium) or as Lipodox (Taro Pharmaceuticals, Haifa, Israel).

Formulation of PLAD:

Most of the experiments presented here were conducted with 2 large batches of PLAD (0.5-1.5 liters) prepared at Nextar Chempharma (Ness Ziona, Israel) following a process similar to that reported previously **(12)** utilizing an 250 mM ammonium alendronate gradient in the same way as the classical ammonium sulfate gradient of PLD resulting in effective and stable loading of Dox in liposomes (11). Vesicle size was measured using dynamic light scattering (DLS) on a Malvern Zetasizer (Malvern, UK). Zeta potential measurements were performed at 25°C using a Malvern Zetamaster (Malvern, UK). Liposome samples were imaged using cryo-transmission electron microscopy (cryo-TEM). Sample preparation and examination by cryo-TEM was carried out at the Hebrew University Center for Nanoscience and Nanotechnology (Jerusalem, Israel), on a FEI Tecnai 12 G2 TEM, operated at 120 kV. Further details of formulation methodology are as previously reported (11). In a few experiments, we used small batches of PLAD (~50 ml) prepared in our laboratory as described before **(12)**.

A summarized description of the formulation of PLAD follows. The PLAD formulation is prepared by the standard method of ethanol injection into an aqueous buffer containing a salt of ammonium alendronate (passive encapsulation), followed by extrusion, buffer exchange, and remote gradient loading of Dox based on a previously described method (12). The lipid components: HSPC, mPEG-DSPE, and Chol at 55%, 40%, and 5%, molar ratios respectively, are dissolved in warm (60°C) ethanol. This ethanol lipid solution

is then mixed with an aqueous buffer of 250 mM ammonium alendronate salt, prepared by mixing a solution of 250 mM alendronic acid with ammonium hydroxide (25%) with a pH in the range of 6.2-6.8. After mixing and shaking for 1 hour at 60°C, the multilamellar vesicles obtained are downsized by serial extrusion in a high-pressure extruder (Lipex Biomembranes, Vancouver, BC), at 60°C through double stacked polycarbonate 0.08 μm pore size membrane filters. Nonencapsulated Ald and residual ethanol are removed by tangential flow filtration (TFF) against a dextrose/Hepes buffer (5% dextrose with 17 mM sodium HEPES, pH 7.0). The liposomes are then remote loaded with Dox with a gradient generated by ammonium alendronate (**Fig. 1A**) by mixing with a solution of 10 mg/ml Doxorubicin HCl in dextrose/Hepes buffer, and incubating for 30 min at 60°C. Non-encapsulated Dox is removed by TFF. The liposome suspension is clarified by filtration through 0.45/0.22 μm-pore cellulose membranes. Doxorubicin concentration is then measured and its final concentration in the formulation is adjusted to 1.0 mg/mL by further dilution with dextrose/Hepes buffer, after which the liposome product undergoes final sterilization by filtration through 0.22 μm-pore cellulose membranes.

Stability assays:

Formulation stability was assessed based on exposure to either pooled expired human plasma as previously described (11) or to human serum albumin (HSA) from commercial sources. We have recently introduced this test based on exposure of liposomes to albumin due to the need for a standardizable stability assay for release of liposome batches for clinical use. The HSA-based liposome stability test is preferable over the plasma stability test. HSA is regulated as a biological pharmaceutical product, can be obtained in aqueous solution, lyophilized or more recently as a recombinant product (Leveraging GMP-Grade Human Serum Albumin for Pharmaceutical Manufacturing (pharmasalmanac.com)). HSA lots are well characterized and have uniform composition from lot to lot with a minimal content of impurities. The stability assay itself is similar to the former assay in plasma. We use a concentration range of 5% to 20% HSA, which upon dilution after mixing with liposomes results in a final concentration of 4% to 16% HSA. This range covers the physiologic concentration of albumin in plasma (4 grams %) and above.

In vitro uptake and cytotoxicity assays:

Uptake and cytotoxicity were tested on a variety of human and mouse carcinoma cell lines. Cells were plated and incubated with free or liposomal drugs for the measurement of uptake and cytotoxicity as described in prior references **(12, 19)** and in the Results section.

Animal studies:

Female inbred BALB/c and outbred Sabra mice, 8–10 weeks old, were obtained from Harlan Biotech (Jerusalem, Israel). *In vivo* experiments were performed either at the Shaare Zedek Medical Center Animal Lab or at the Animal Facility of the Hebrew University-Giv'at Ram Science Campus. Animal experiments conducted in Israel were approved by the Animal Ethics Committee of the Hebrew University–Hadassah Medical School. Animal experiments conducted in the UK were ethically reviewed and carried out in accordance with the Animals (Scientific Procedures) Act 1986 (ASPA) UK Home Office regulations governing animal experimentation with local approval from King's College London Research Ethics Committee. For further details on animal studies and tumor models, see relevant sections of Results.

Determination of Dox in PK and biodistribution assays:

Mice were injected i.v. with an equal dose of free Dox, PLD or PLAD based on doxorubicin content. For blood collection, mice were anesthetized by halothane or isoflurane

inhalation, bled by eye enucleation (~1ml blood per mouse) and immediately after sacrificed by cervical dislocation. Blood was collected in heparinized tubes and centrifuged immediately to separate plasma from blood cells. Plasma levels of doxorubicin were measured fluorometrically after extraction from plasma with acidified isopropanol as described previously **(20)**. Tissue biodistribution was assessed either in tumor-free or tumor-bearing mice. Tumors were generated by subcutaneous inoculation of tumor cell suspensions in the flanks or in the inter-scapular space.

Preparation of radiolabelled PLAD ([^{111}In]In-PLAD) and formulation:

[^{111}In]In-PLAD was radiolabeled as previously reported in similar PEGylated liposomes *(21)* using an ionophone approach with [^{111}In]In(oxinate)$_3$ produced using the chloroform method *(22)*. The final formulation injected per mouse contained 50 μg radiolabeled PLAD liposomes and plain (drug-free) HSPC/CHOL/mPEG2000-DSPE liposomes (FormuMax, UK) with similar lipid composition to PLAD to a total 4 μmol of lipids in 130-150 μl of PBS.

SPECT/CT imaging study with ex vivo biodistribution and tumor autoradiography:

We conducted an imaging study in a WEHI-164 subcutaneous mouse tumor model. After 10-14 days of subculturing, WEHI-164 cells were harvested and two million cells were inoculated subcutaneously unilaterally in the shoulder of BALB/c mice 8-9 weeks-old (Charles Rivers, UK). On day 9 after inoculation the mice were injected i.v. by tail vein bolus injection with ca. 10 MBq [^{111}In]In-PLAD. Mice underwent SPECT /CT imaging at 30 min, 24h, 48h, and 72h post-injection. SPECT imaging was performed with a four-headed multiplexing multipinhole NanoSPECT/CT (Mediso, Hungary) using Aperture 3 (1 mm pinholes). A 96 mm field of view comprising the animal from tip of the nose to end of the back legs was used with an energy peak of 171 and 245 KeV ± 10% keV. The acquisition time was adjusted ranging from 40-80 s, increasing it to compensate for the isotope decay in later timepoints. A 21 min 360 frame CT imaging was performed immediately before or after the SPECT acquisition. Reconstruction of the images was performed including attenuation correction using the software HiSPECT (Invicro, USA) with standard parameters. Reconstructed data from SPECT and CT were co-registered using ViVoquant (Invicro, USA) for further analysis and interpretation.

For analysis of ex vivo biodistribution after completion of imaging, the tissues were collected, weighted and counted in 1282 CompuGamma gamma counter (LKB Wallach, Sweden), alongside standard samples of known radioactivity. For autoradiography studies, tumors where snap frozen and cut in 45 μm slices for autoradiography. The tumor slices were set against imaging plates (GE, UK) for 3 days and autoradiograms were obtained using an Amersham Typhoon 5 (GE, UK) analyzer system with a resolution of 25 μm and sensitivity of PTM of 4000.

Toxicity studies:

These studies were done in tumor-free BALB/c mice receiving weekly i.v. injections of PLD or PLAD. Mice were observed and weighed weekly x3 and followed for up to 60 days.

Antitumor efficacy:

BALB/c female mice (~8-10-week-old) were inoculated with M109R mouse tumor cells (10^6 cells) or Wehi-164 mouse tumor cells (10^6 cells) s.c. in the left or right flank. In the 4T1 model, tumor cells (10^5 cells) were injected in the right hind footpad. When tumors became palpable, free drug or liposomal drug treatment were injected i.v. in the tail vein, while anti-PD1 mouse antibodies were injected i.p. according to the schedule of each specific experiment. Mice were monitored at least twice per week for body weight and for tumor

size with precision calipers. Tumor growth was followed for up to 60 days. Statistical analysis was done using Prism software version 9 (Graphpad, San Diego, CA).

Therapeutic studies combining PLAD with gamma-delta T cell transfer:

These experiments were done as described previously for a human epithelial ovarian cancer model **(23)** treated with gamma delta (subset Vγ9 Vδ2) T cells, except that the tumor model used here was the MDA-MB-231, a triple negative human breast cancer model and in addition to PLA, PLAD was also tested. Gamma delta T cells were obtained from blood cells of healthy donors, expanded *in vitro* and collected for the *in vivo* studies as described previously **(23)**.

3. Results

Formulation and characterization of PLAD

For details on the PLAD formulation process, see the Methods section above. The concentrations of the liposome components of PLAD for two successive batches are listed in **Table 1**. All values obtained fell within a pre-specified target range considered to be acceptable for batch release. The potency of the formulation is based on the Dox content of PLAD, which is measured by a previously described HPLC assay (12). Ald concentration is based on phosphorous assay of the upper phase of a Folch extraction of the liposomes as described previously (11). PLAD average vesicle size, as measured by dynamic light scattering, is 90-100 nm with narrow polydispersity (PDI<0.15). CryoTEM photographs of the PLAD formulation reveal spherical vesicles with intravesicular packs of rods resulting from crystallization of the Ald-Dox complexes. Unlike PLD, no oval-shaped liposomes are seen in PLAD, and the PLAD rods appear to be shorter and more loosely packed than the Dox-sulfate rods of PLD (**Fig 1B).**

Table 1. Characteristics of PLAD batches used in this study.

PLAD Batch (batch size)	Vesicle Size nm	PDI	Zeta potential mV	Osm. mOsm/kg	pH	ALD mg/g	Cholesterol mg/g	mPEG2000-DSPE mg/g	HSPC mg/g	DOX-HCl mg/g[1]
Batch 1 (0.5 L)	110.3	0.058	-12.13	317	7.1	0.5	1.62	1.36	4.6	0.9
Batch 2 (1.5 L)	99.8	0.028	-13.41	291	6.7	0.6	1.62	1.21	4.3	0.9

[1] The potency of the batch is labeled as 1 mg/ml of Dox-HCl equivalents (acceptable range 0.9-1.1). The actual result in these 2 batches is 0.9 mg/g or ml.

Upon storage at 4-8°C, PLAD is highly stable in aqueous buffer suspension retaining >97% of Dox in encapsulated form with vesicle size remaining stable for >18 months. In the past we have used Sepharose columns to separate released free drug from liposomal drug *(12)*. A more convenient and accurate method to follow up for stability of encapsulation is centrifugation of a liposome sample using Vivaspin® ultrafiltration tubes (Sartorius, UK) with the appropriate MW cutoff (300 Kd) such that only free drug passes through the filter and can be quantified by the relevant methods, phosphorus assay for Ald and fluorescence assay for Dox. Based on this assay and on DLS particle size analysis, we found no significant leakage of Dox or Ald and no significant change in vesicle size and polydispersity suggesting that these critical parameters of the PLAD formulation are stable over the course of ~2 years (data not shown).

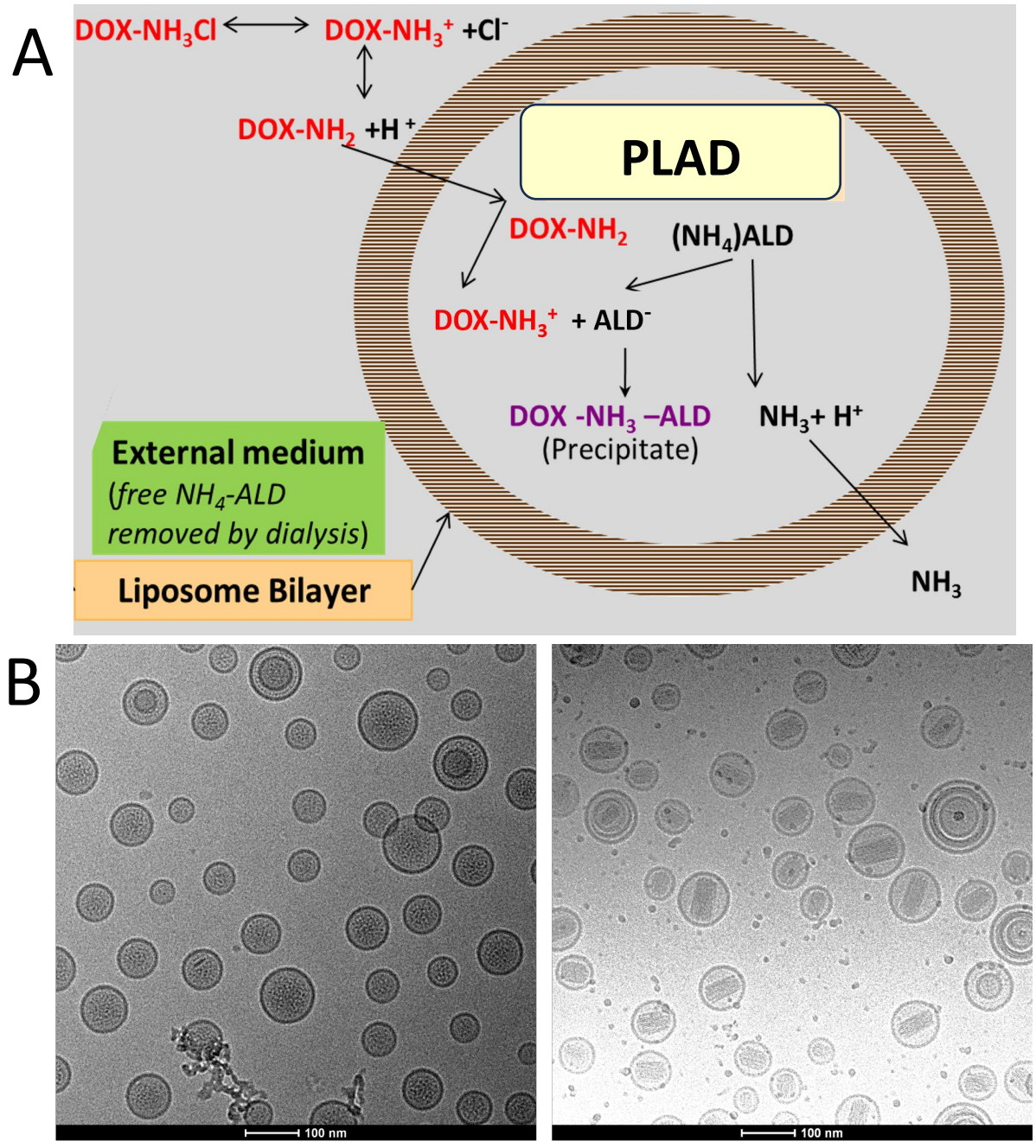

Figure 1. A. Schematic drawing of doxorubicin loading using an ammonium alendronate gradient for co-encapsulation to form Pegylated Liposomal Alendronate salt of Doxorubicin (PLAD). **B.** Comparative cryoTEM view of alendronate-containing liposomes before (PLA) and after loading with Dox (PLAD). Left panel (PLA): spherical liposomes with few MLV; Right panel (PLAD): spherical liposomes with thick rods of precipitated Dox, and few MLV.

Stability of PLAD in biological fluids:

The stability of the PLAD formulations was assessed in vitro with a plasma stability assay by exposure to human plasma for 2 h at 37°C. This test gives a good prediction of

the degree of stability *in vivo* in circulation, although it has serious limitations as a standard test for drug development because of the variability of plasma sources which is usually obtained from expired batches of fresh frozen plasma before they are discarded from the blood bank.

We have shown in the past that no leakage of Ald occurs in plasma (12). In fact, Ald is very hydrophilic and cannot cross a cholesterol-rich solid bilayer at 37°C, as in the case of HSPC-containing PLAD liposomes. In addition, most of the Ald is complexed with Dox and precipitated in the liposome water phase. Release of Ald requires first dissociation from doxorubicin complex and then a breakdown of the liposomal bilayer integrity. Unlike Ald, Dox may leak from liposomes if the proton gradient is lost because of its amphipathic nature, even if the liposomal bilayer remains intact. We, therefore, chose to examine leakage of Dox as a surrogate marker of liposome stability in biological fluids.

Fig. 2A shows the release of Dox in fractions of eluent collected from a Sepharose column after incubation of the liposomes in human plasma and in buffer. Nearly all the drug remain liposome-associated form and elutes together with liposomes in fractions 4-6, while plasma proteins elute mostly in fractions 7-11. There was a minor and insignificant difference between the elution profiles in plasma and buffer. This indicates that drug leakage in plasma is minimal and probably insignificant.

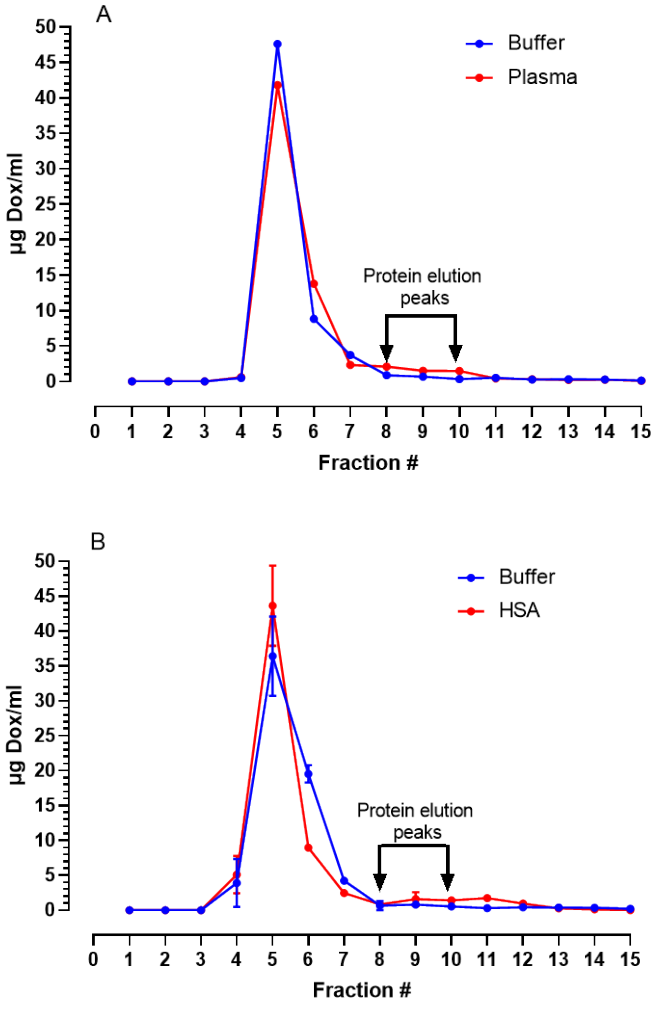

Figure 2. A. Stability of PLAD incubated in 80% human plasma; **B.** Stability of PLAD incubated in HSA at a concentration of 4 g%. Liposomal drug peak elutes in fractions 5-6, proteins in fraction 8-

10, and free drug in fractions 11-12, indicating that Dox remains associated with the liposome fraction, no significant leakage detected.

As an alternative to plasma, we have used commercial sources of human serum albumin (HSA) which is well characterized and has uniform composition from batch to batch. As seen in **Fig. 2B**, incubation of PLAD in 4%-16% HSA under the same conditions as plasma resulted in negligible leakage of Dox, indicating that PLAD is highly stable when exposed to a protein-rich fluid and maintains the gradient that holds the drug in the vesicle interior.

In vitro cell studies with PLAD: uptake and cytotoxicity

Dox uptake studies in a variety of tumor cell lines indicate great variability of liposomal drug uptake but, along with that, there was a trend to higher uptake of PLAD when compared to PLD in all cell lines (**Fig. 3A**). Since drug leakage is negligible under these conditions for both formulations, the uptake of Dox is probably related to the number of vesicles taken up by the cells. The Dox/phospholipid ratio is higher in PLD than in PLAD and therefore cannot explain this difference in drug uptake. It is tempting to speculate that these small differences may be related to other characteristics such as differences in vesicle shape, aspect ratio or membrane rigidity between PLAD and PLD *(24)*.

We also looked at liposome uptake when raising temperature to 42°C in KB cells, a cell line which has a high endocytic activity for liposomes. Interestingly, as seen in **Fig. 3B**, liposomal drug uptake was greatly increased with both liposomal formulations (18 to 24-fold) as compared to free drug (~4-fold). PLD and PLAD are both high Tm liposomes which are unlikely to leak drug at temperatures below 50°C. This has been confirmed in experiments with grafting of ligands onto Dox pre-loaded liposomes at 45°C *(25)*.

Therefore, the increased uptake of liposomal drug with a moderate rise of temperature is probably related to an increase of endocytic activity. If these observations, are confirmed in vivo, they may have translational relevance and support the use of liposomal drugs, rather than free drugs, with regional hyperthermia.

As expected, PLAD and PLD were much less cytotoxic than free Dox which is always the case in vitro for stable liposome formulations (26).The in vitro cytotoxicity of PLAD is consistently superior to that of PLD on several mouse and human carcinoma cell lines (**Table 2**, see also growth inhibitory curve in supplement Fig. S1) with a broad variation in sensitivity to Dox. This increased cytotoxicity may be the result of the slight increase of in vitro uptake of PLAD as compared to PLD **(Fig. 3)**. A simple additive effect of Ald is unlikely since free Ald and more so liposomal Ald has little or no in vitro cytotoxic effect in the pharmacological concentration range (12, 27). However Ald may sensitize the cells to Dox, once it becomes available in the intracellular compartment, through the inhibition of the mevalonate pathway at the level of FPP synthase (28). This will translate in synergistic cytotoxicity of PLAD as shown for another aminobisphosphonate encapsulated in nanoparticles *(29)*.

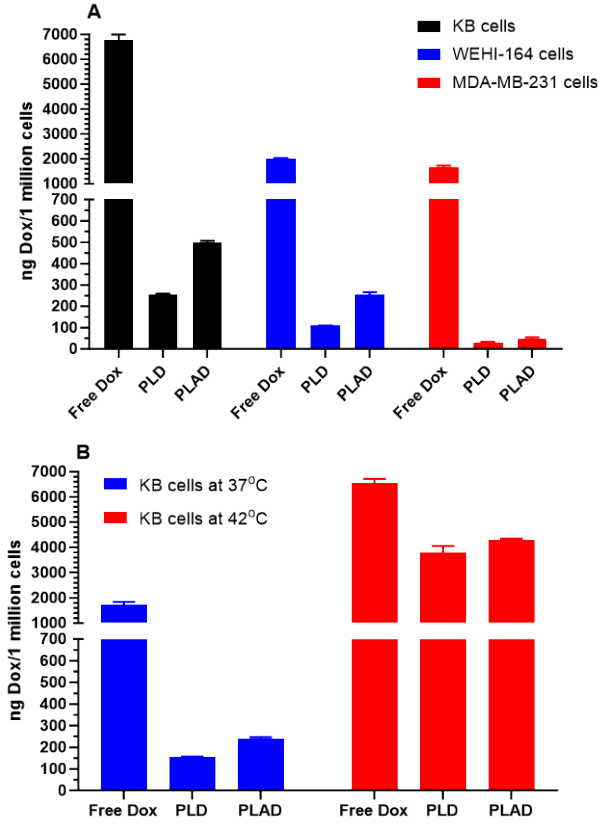

Figure 3. A. *In vitro* drug uptake by tumor cells exposed to free Dox, PLD, or PLAD at 37°C for 3 h. As expected, free drug is taken at much higher levels than liposomal drug. The uptake of liposomal drug per 10^6 cells varies widely between the different cell lines, with a slightly greater uptake for PLAD than for PLD in KB and Wehi-164 cell lines. **B.** Effect of temperature increase to 42°C on drug uptake by KB tumor cells exposed to free Dox, PLD, or PLAD for 3 h. Drug uptake increased with temperature by 3.8-fold for free Dox, 24.2-fold for PLD, and 17.8-fold for PLAD.

Table 2. *In vitro* cytotoxicity studies with Free Dox, PLD and PLAD in human and mouse tumor cell lines[1].

Cell line	KB	MDA-MB-231	Wehi-164	4T1	M109
Free Dox	0.07	0.6	0.5	2.2	0.1
PLD	4.8	15.9	18.75	>50	8.0
PLAD-1	0.6	5.1	4.6		1.0
PLAD-2	2.0	11.7	6.6	24.6	
Free Ald			>50		

[1] Representative results from n=1-4 experiments per cell line

.

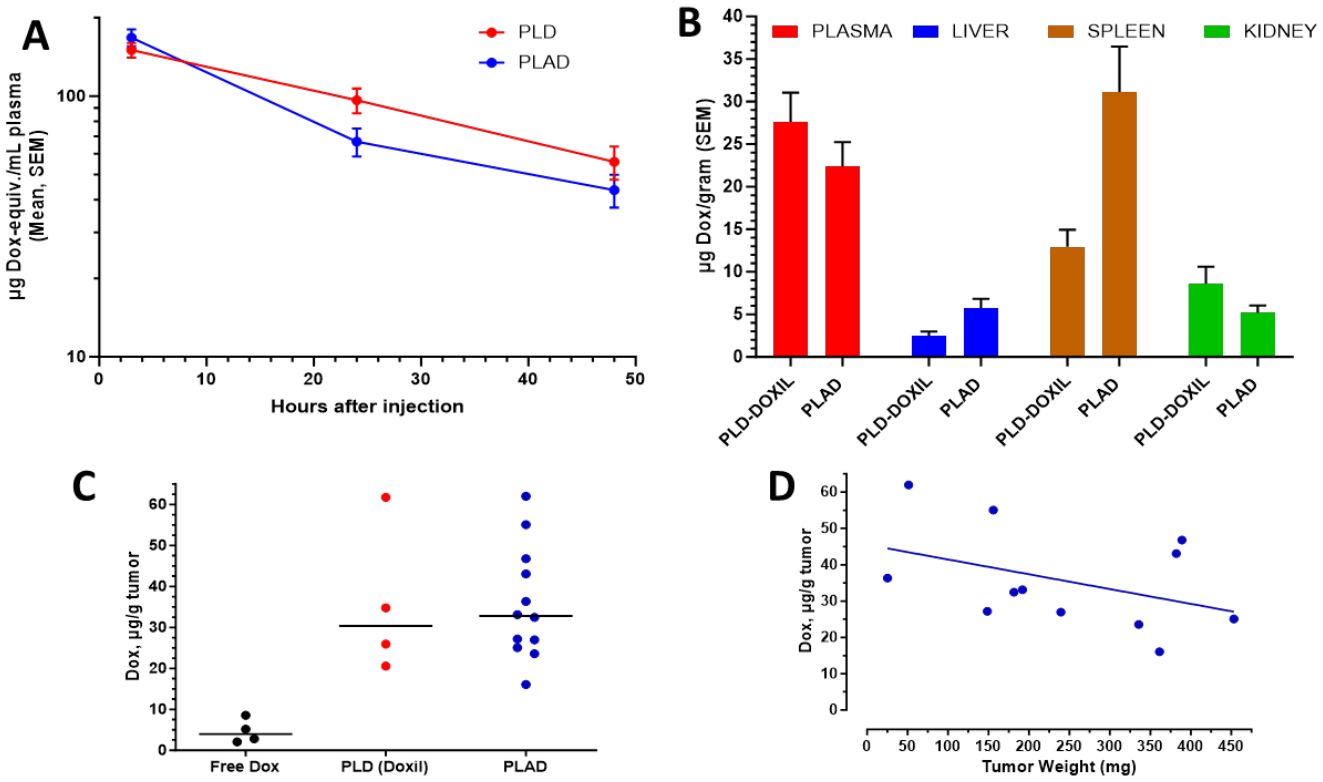

Figure 4. Pharmacokinetics and biodistribution of PLAD and PLD in M109 tumor-bearing BALB/c f mice after i.v. injection at a dose of 10 mg/kg. **A.** Plasma Dox levels are slightly lower for PLAD than for PLD with a long circulation half-life of ~24 h in both cases. **B.** Tissue distribution at 72 h post-injection reveals greater liver and spleen drug levels and slightly lower blood levels for PLAD as compared to PLD. **C.** Tumor drug levels are roughly equivalent for PLD and PLAD and much greater (~10-fold) than in free Dox injected mice. **D.** Linear regression plot showing a non-significant trend of lower tumor drug uptake per gram when tumor weight increases.

Pharmacokinetics and Biodistribution:

PLAD demonstrated a prolonged circulation time in mice, slightly lower than PLD (**Fig. 4A)** with a difference of minimal significance, based on total plasma Dox concentrations**.** The tissue Dox levels were increased moderately in liver and markedly in spleen and somewhat decreased in kidneys when PLAD is compared to PLD (**Fig. 4B**). As previously observed in the Wehi-164 model *(18)*, we found a non-significant increase of the tumor drug content when PLAD is compared to PLD in the M109 tumor model. Both liposome formulations dramatically increased the amount of Dox measured in tumor tissue when compared to free Dox (**Fig. 4C**). An additional observation in PLAD-injected mice, similar to what as be reported with PLD (30), was a non-significant trend to lower drug levels per gram tumor as the tumor size increases (**Fig. 4D**).

Imaging studies of PLAD in tumor-bearing mice:

To further investigate the biodistribution of PLAD in tumor-bearing mice, we conducted an imaging study (SPECT-CT) in BALB/c mice inoculated with the WEHI-164 tumor model. As indicated in the Methods section, PLAD was radiolabeled with the gamma-emitter indium-111 (^{111}In) using a previously published method *(21)* to form [^{111}In]In-PLAD. Each mouse received a total dose of 4 μmol of lipids by combining [^{111}In]In-PLAD with empty liposomes of the same composition and physicochemical properties (size and zeta potential) but lacking doxorubicin/alendronate. After intravenous injection, mice were imaged by SPECT-CT (**Fig. 5A**) for up to 72 h, and, at the end of the study, an ex-vivo biodistribution of analysis in mice injected with [^{111}In]In-PLAD was performed (Figure 5B).

The study revealed high and heterogeneous accumulation of PLAD in the tumor (Fig. 5A), with an average uptake value of 40.4 ± 28.7 % Injected Activity (IA)/g at 72h and a highest tumor uptake value of 101 % IA/g in a very small tumor. As expected from previous biodistribution data in mice, the spleen was the organ that had the highest uptake at this timepoint followed by the tumor and liver (**Fig. 5B**). Further analysis of the results indicates a higher uptake in tumors of smaller size in comparison with larger ones (**Fig. 5C**) as suggested for liposomal drug in Figure 4D and consistent with previously published observations on liposome biodistribution (31). The intratumoral distribution was heterogeneous, with a higher concentration of radiolabeled PLAD at the edge of the tumor, as observed via autoradiography studies of small slices of tumor tissue (see inset in Fig. 5A).

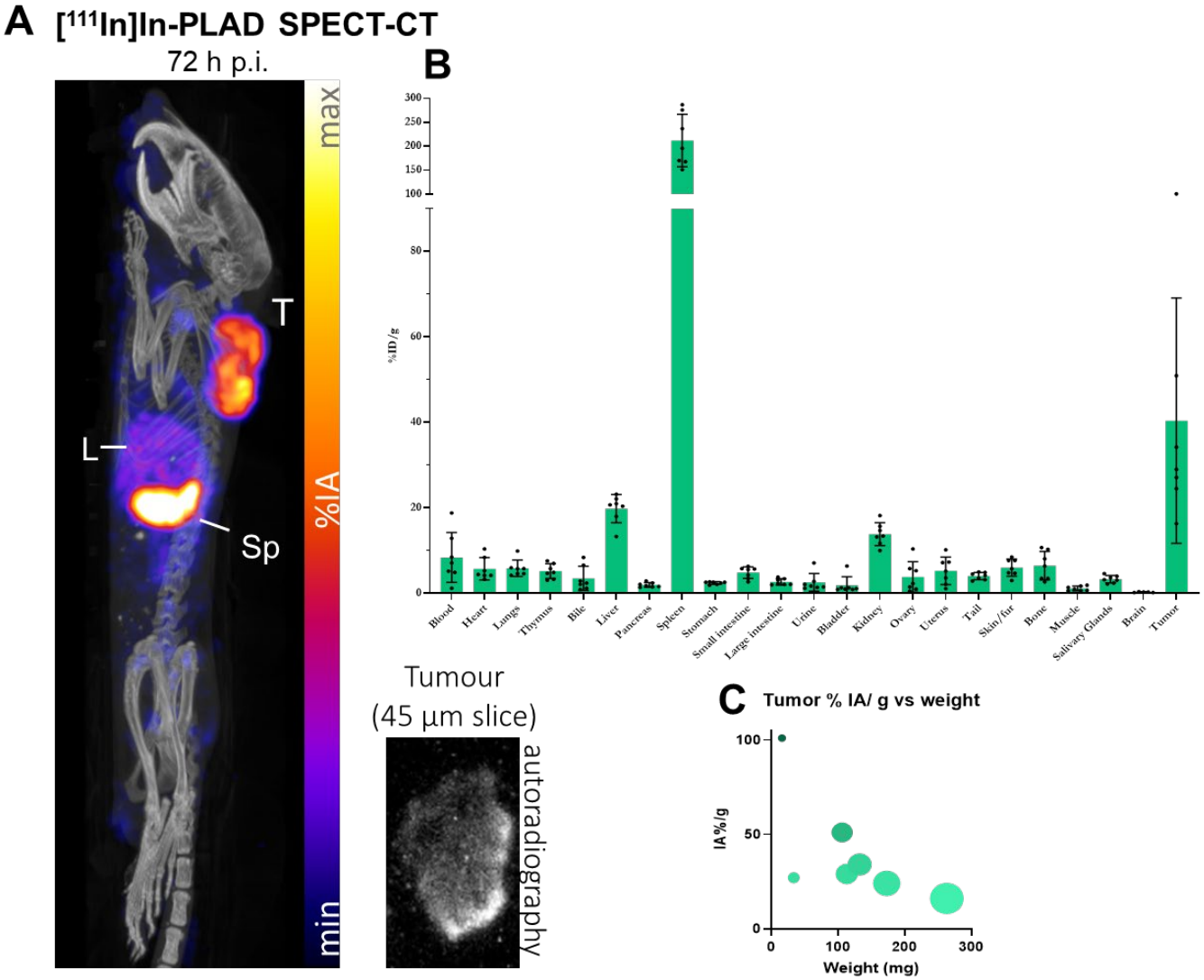

Figure 5. A. Representative images showing SPECT/CT imaging (maximum intensity projection) and autoradiography of a 45 µm tumor slice after 72 h post iv injection of [111In]In-PLAD. (T = tumor; L = liver; Sp = spleen; H = heart/blood pool); **B.** Ex vivo biodistribution of [111In]In-PLAD at 72h post injection; **C.** A comparison between tumor uptake of [111In]In-PLAD in all tumors vs their respective mass at 72 h post injection.

Toxicity study

An experiment comparing the toxicity of PLD and two batches of PLAD in tumor-free outbred Sabra female, 7-week-old, mice. Mice were injected i.v. with a dose of Dox close to the maximal tolerated dose of PLD, 10 mg/kg, in two successive weekly injections and followed for 6 more weeks. As seen in **Fig. 6**, the weight curves of PLAD-injected mice rose shortly after treatment unexpectedly suggesting fluid accumulation and then dipped but not more than 15%. One mouse out of 8 injected with PLAD died on day 14. Hair loss was also noted in one mouse injected with PLAD. All other mice survived, recovered and gained weight normally. The weight gain of PLD-injected mice was transiently affected but otherwise, there was no other sign of toxicity. Based on these results, PLAD seems to be slightly more toxic than PLD. We therefore chose to conduct therapeutic studies with dose levels ≤ 8 mg/kg in immunocompetent mice.

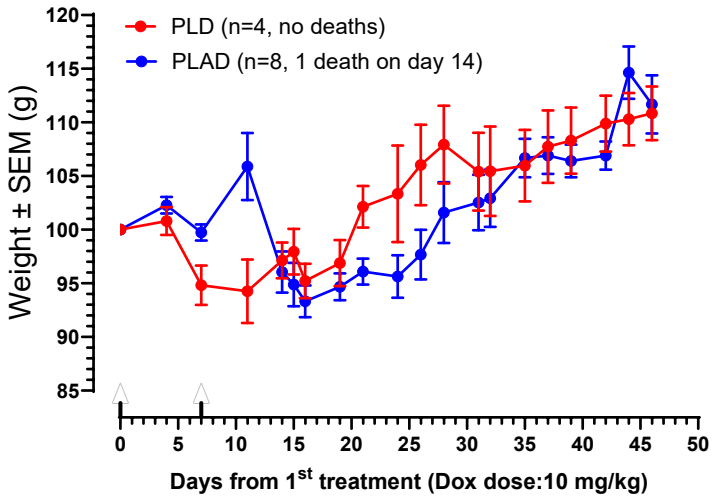

Figure 6. Comparative toxicity of PLD and PLAD in tumor-free Sabra f mice by weight curves. PLD and PLAD injected i.v. at a dose of 10 mg/kg in two successive weekly injections. Mice were weighed at least 2x per week and inspected 3x per week.

Therapeutic activity of PLAD:

Our former observations in the M109R and 4T1 tumor models in immunocompetent mice (12) were reproduced with the current optimized formulation of PLAD. PLAD was superior to PLD in these models. In the 4T1 tumor model, a significant number of complete tumor regressions or cures was achieved with PLAD (5/9) compared to PLD (1/9) (**Fig. 7A-C**). In addition, we conducted therapeutic studies in the WEHI-164 mouse sarcoma model. In this highly Dox-sensitive model, PLAD and PLD demonstrated great efficacy with complete tumor regression in 100% and 90% respectively of mice inoculated with the WEHI-164 sarcoma model implanted subcutaneously in BALB/c mice. Free Dox treatment was also highly efficacious but resulted in fewer (70%) complete tumor regressions (**Fig. 7D-G**).

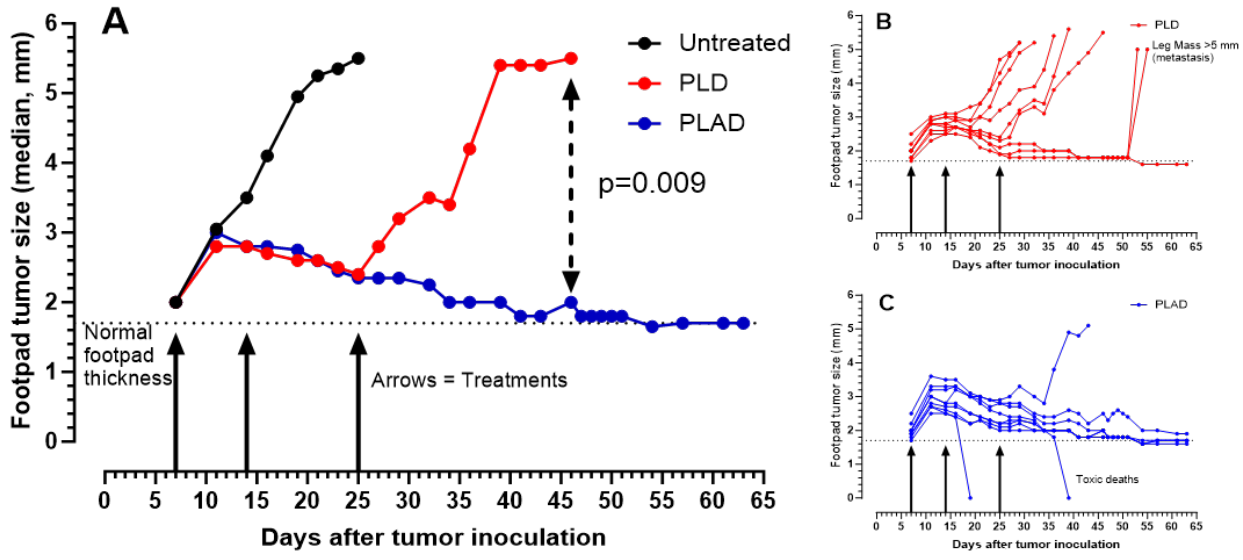

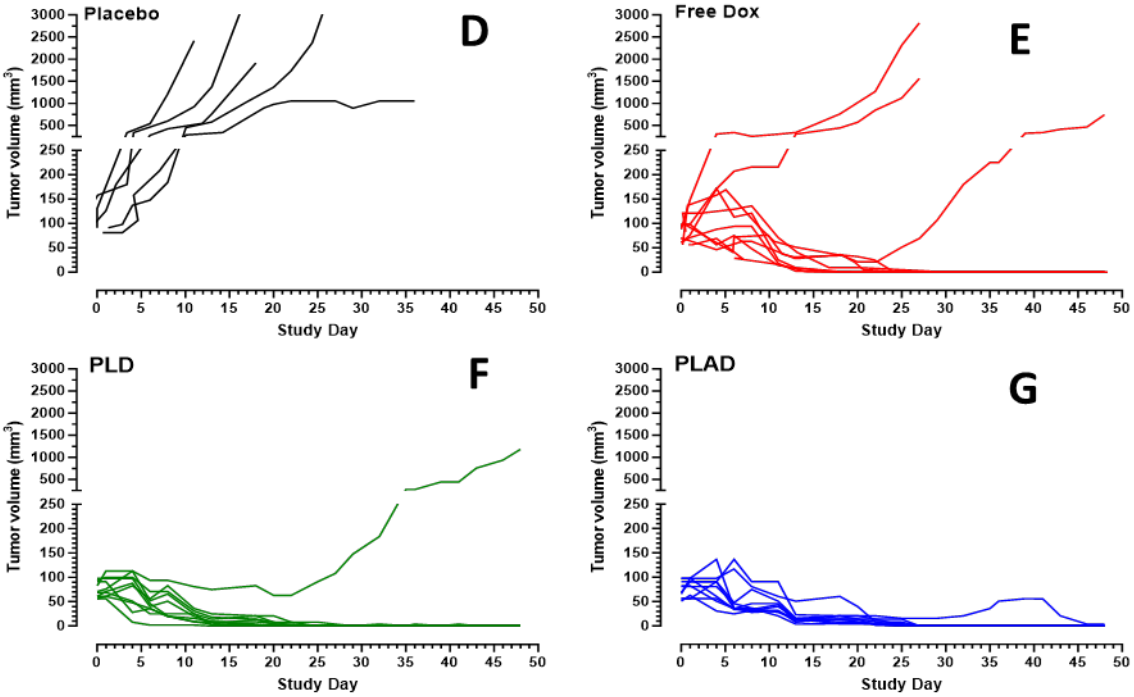

Figure 7. Therapeutic activity of PLAD in 4T1 and WEHI-164 mouse tumor models. **A-C.** 4T1 model: BALB/c inoculated with 10^5 471 tumor cells s.c. (intra-footpad). PLD and PLAD injected i.v. at a dose 8 mg Dox/kg on days 7, 14 and 25. Individual tumor growth curves for PLD and PLAD are presented in panels **B** and **C.** There were 2 toxic deaths in the PLAD group. At end of study 5/9 mice in the PLAD group were free of tumor compared to 1/9 in the PLD group. **D-G.** WEHI-164 model: BALB/c mice inoculated with 10^6 Wehi-164 cells s.c. when tumors reached an estimated volume of 50-100 mm^3, mice were treated with Placebo (PBS), Free Dox, PLD, or PLAD at a dose of 6 mg/kg weekly x3. Panels **D-G** present the individual tumor growth curves for each of the treatment groups. All treatments were very effective although PLAD was the only treatment achieving complete regressions in 100% of the mice. The difference between PLAD and Free Dox curves by the log rank test was borderline significant (p=0.0671).

We then explored the therapeutic activity of PLAD and PLD in combination with a mouse anti-PD1 antibody in the Dox-resistant M109R tumor model. A seen in **Fig. 8**, treatment with PLAD and anti-PD1 resulted in the best outcome with the smallest tumors observed at end of study. Free Dox is ineffective in this highly multidrug resistant tumor model (32).

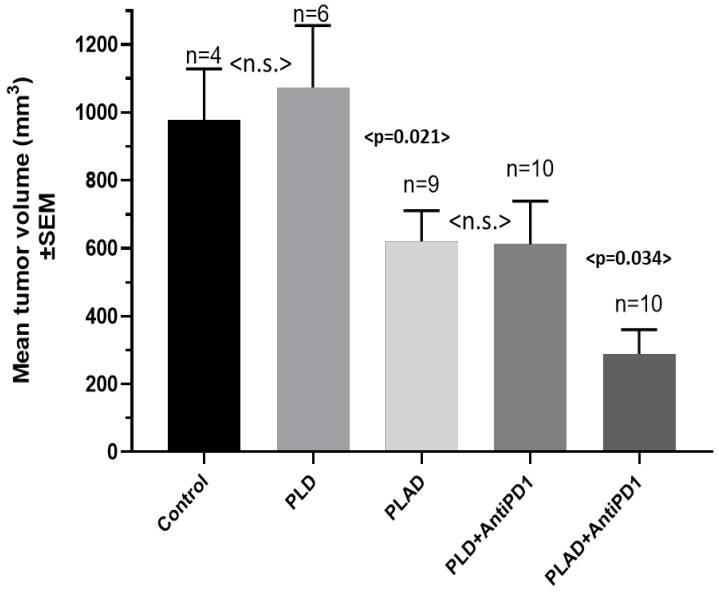

Figure 8. Anti-tumor activity of PLAD and PLD with or w/o immune checkpoint inhibitors (anti-PD1) in a mouse MDR tumor model (M109R). BALB/c f mice inoculated s.c. with 10^6 M109R tumor cells. Once tumors became palpable, mice were treated i.v. with 2 weekly injections of PLD or PLAD at a dose of 8 mg/kg, with or without anti-PD1 at a flat dose of 200 μg per mouse by i.p. injection. On day 40, mice were sacrificed, tumors dissected and weighed. Mean tumor weight per treatment group were calculated. Statistical analysis (Mann-Whitney Test): PLD+antiPD1 vs PLD, p=0.0460; PLAD vs Untreated, p=0.0539; PLAD vs PLD, p=0.0211; PLAD+antiPD1 vs Untreated, p=0.0040; PLAD+antiPD1 vs PLD, p=0.0069; PLAD+antiPD1 vs PLD+antiPD1, p=0.0340; PLAD+antiPD1 vs PLAD, p=0.0144. All other comparisons were not significant.

PLAD and gamma-delta T cells:

Our previously published work with PLA in combination with adoptively transferred gamma-delta (Vγ9 Vδ2) T lymphocytes from human donors in an in vivo human tumor model demonstrated a significant antitumor effect of this combination *(23)*. Moreover, PLA was shown to increase the number of infused gamma-delta T cells localizing in tumors (33). Subsequent in vitro studies with human breast cancer and AML cell lines indicated that PLAD is a strong activator of gamma-delta T cells (US Patent #10,085,940, Gabizon et al., Liposomes co-encapsulating a bisphosphonate and an amphipathic agent, issued Oct 02, 2018).

We therefore conducted experiments to investigate the activity of PLAD in combination with human gamma-delta T cells in a human breast cancer mouse tumor model. As seen in **Fig. 9A-B,** the best therapeutic outcome was seen with the combination of gamma delta T cells and PLAD in combination with human gamma-delta T cells. PLAD alone was also highly active but Vγ9 Vδ2 T lymphocytes as single modality treatment or in combination with PLA were clearly less effective. No significant toxicity (weight loss, general appearance) was observed when PLAD was combined with gamma-delta T cells in the course of the experiment. For a detailed figure with all weekly measurements of bioluminescence, see supplement Figure S2

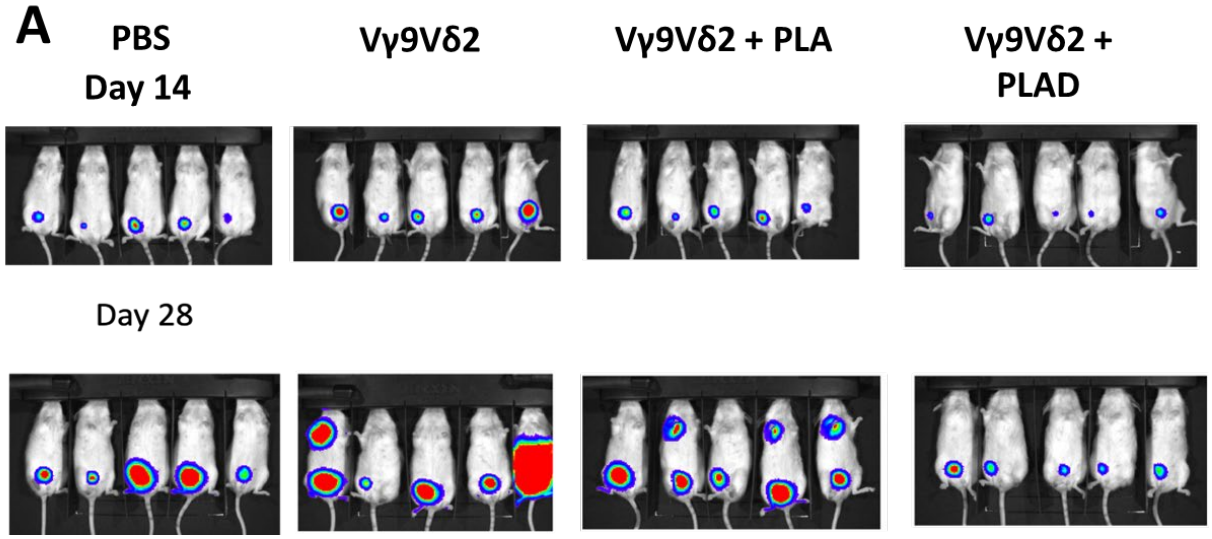

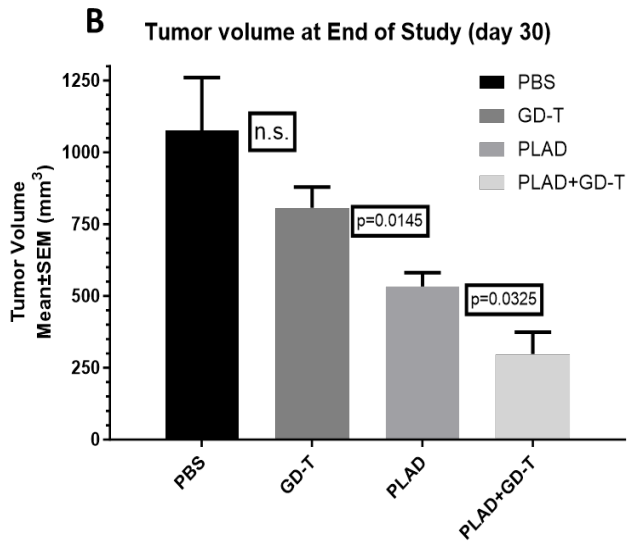

Figure 9. Anti-tumor Effect of PLAD in combination with antitumor gamma delta T cells in a triple negative human breast cancer mouse model. **A.** SCID Beige mice were inoculated with 10^5 MDA-MB-231(luc) tumor cells into lower mammary fat pad. When tumors became palpable, groups of 5 mice each were injected i.v. with PBS control, no treatment, low dose PLA (5 mg Ald/kg), high dose PLA (8 mg Ald/kg) or PLAD (5 mg Dox/kg). 72 hours later, all mice, except for PBS group, received by i.v. injection $8x10^6$ gamma-delta T-cells per mouse. Bioluminescence imaging (BLI) was followed weekly after i.p. injection of 200 µl luciferin as previously done (19). Lymph node metastases can be noticed in some mice injected with PLA and gamma-delta cells. **B.** A second experiment was done with the same tumor model to compare efficacy of PLAD with or without gamma delta T cells. In this study, $2x10^7$ gamma-delta T-cells were injected 24 h after PLAD 5mg Dox/kg. Mice were culled on day 30 after treatment start, tumors dissected and weighed. PLAD with gamma delta T cells was clearly the most effective treatment. See *p* values (*t* test) in 9B.

4. Discussion

Co-encapsulation in a stable nano-formulation of two active agents preferably with non-overlapping toxicities and synergistic effects is a unique advantage of nanomedicines. By space and time co-delivery of two drugs with otherwise different pharmacokinetic-biodistribution profiles, we can exploit combination therapy at its best and achieve

optimal synergistic activity. As mentioned in the Introduction section, a clinical example is a liposome-based formulation of cytarabine and daunorubicin at an optimized 5:1 drug-to-drug ratio, known as Vyxeos™, approved for treatment of adult AML (34). In this formulation the liposome carrier controls and nearly equalizes the pharmacokinetics of both drugs (35). There are other examples of co-encapsulated drugs in liposome and polymeric formulations with positive results in animal models (36-38). However, in most instances, co-encapsulation consists of 2 cytotoxic drugs in contrast to our PLAD formulation in which two drugs with non-overlapping mechanisms of action and toxicity profiles are co-encapsulated. While this approach is pharmaceutically and regulatory-wise challenging, it is a unique advantage of nanomedicine and beholds promise for future applications (30).

The starting point for the formulation if the well-known PLD formulation approved for ovarian and breast cancer and widely used in the clinic for more than 20 years with a great safety record (13). Despite the important pharmacologic advantages of PLD, its impact and added value on the survival of cancer patients has been modest. A number of reasons have been invoked for this apparent discrepancy between the preclinical and clinical results (13). We hypothesize that nanodrugs, particularly those that deliver immunogenic cell death inducers such as doxorubicin (39), are more suitable and effective than conventional chemotherapy for combination with immunotherapy given their affinity and their putative suppressive effect of tumor-associated macrophages (TAM) which tend to have an overwhelming M2 tumor-promoting effect (40, 41). Therefore, one way to improve the performance of PLD may be through combination with immunotherapy. Clinical studies with combination of PLD and immune checkpoint inhibitors are still at an early phase, but their initial results are encouraging (42-45). In parallel, we postulate that the combination of Dox with an immunomodulator and TAM-suppressor drug such as ALD in the same liposome, as done in PLAD, should improve the synergistic effect with anti-PD1 antibodies and perhaps other checkpoint inhibitors, as suggested by a recent study showing that PLAD has a stronger raising effect on the M1/M2 ratio when compared to PLD (18).

In the said study of Islam et al. (18), PLAD and PLD were found to shift the balance between various immune cell types and their functionality creating changes in the TME conducive to an improved antitumor response (18). These effects were absent in free Dox-treated mice. The effects of PLAD were generally stronger than those of PLD, particularly the association of PLAD with TAM, suppression of TAM activity and relative increase of the ratio of M1 over M2 macrophages. Besides their effects on TAM, treatment with aminobisphosphonates, particularly in liposomal form, results in the formation of phospho-antigens that stimulate a natural immunity response against cancer mediated by Vg9Vd2 gamma-delta T cells. In primates, most circulating gamma-delta T cells express the Vg9Vd2 TCR, enabling their HLA-independent activation and expansion by nonpeptide phospho-antigens (23). This provides a qualitative and unique advantage to Ald-containing liposomes and by extrapolation to PLAD over PLD. Furthermore, treatment with liposomal Ald significantly increased the homing of adoptively transferred gamma-delta T cells to tumors in a mouse model (33).

PLAD offers other advantages in the field of theranostics since Ald is a potent chelator of various metal radionuclides that are used in nuclear medicine for SPECT and PET-CT imaging such as, ^{89}Zr,^{111}In, $^{67/68}$Ga, ^{64}Cu, and ^{52}Mn and hence high potential for other therapeutic radionuclides. This property confers the possibility of tracing reliably PLAD biodistribution noninvasively (46) and perhaps better selecting patients for therapy with PLAD. Nuclear medicine studies with radiolabeled liposomes using modern imaging techniques such as PET-CT or SPECT-CT can be extremely helpful to determine the dose distribution to tumors and to predict response in the individual patient. One distinct advantage of nanomedicine is the possibility of co-encapsulating an active pharmaceutical ingredient (API) with an additional agent that can serve as a radionuclide metal chelator to track the nanoparticle, and thereby the API biodistribution as reviewed by Man et al.

(47). PLAD complies with these requirements since Dox is the main API and Ald is a strong chelator of metals such as ^{111}In or ^{89}Zr (46). In fact, liposome-encapsulated Ald can serve 2 purposes: as an immunomodulating agent working in synergy with the co-encapsulated cytotoxic agent doxorubicin, and as carrier of radionuclides useful for imaging liposome biodistribution. This is in essence a very relevant example of nanomedicine harnessed for improved theranostics.

The enhanced tumor deposition and retention of drugs delivered by long-circulating liposomes has been well established and is referred to as the enhanced permeability and retention (EPR) effect (48-50). Based on the total tumor measurement of liposomal drug, it appears that PLAD has equal or better EPR tumor targeting effect than PLD. Following liposome extravasation and accumulation in tumor tissue extracellular fluid, the fate of liposomes depends on liposome uptake by the various cell types comprising the tumor parenchyma. It has been recognized that nontargeted liposomes are primarily taken up by TAM or remain in the tumor interstitial fluid in the perivascular zone. Tumor cell uptake of liposomes is relatively low although it varies depending on the tumor type. Fortunately, in the case of doxorubicin liposomes, liposomes will gradually lose the gradient and release the encapsulated drug in the tumor extracellular fluid which will thereafter diffuse into surrounding tumor cells and damage them. In this regard, we have recently reported in dissociated tumors that the tumor cell-associated liposomal drug is significantly greater for PLAD than for PLD (18). This interesting finding may be explained by a faster drug release form PLAD in tumors or by PLAD-induced suppression of TAM activity (51) which may allow for more liposomes to be available for tumor cell uptake.

It is increasingly recognized that therapy aimed at killing cancer cells (i.e., cytotoxic chemotherapy) is insufficient for inducing durable cancer remissions, and that mobilization of the adaptive immune response against cancer cells is necessary. Immunotherapies such as the immune checkpoint inhibitors can produce complete remission in metastatic cancer patients who remain relapse-free for years (52, 53). Nonetheless, immune checkpoint blockade as a single treatment modality is only efficacious in a small subset of patients often due to the low tumor immunogenicity and TAM-induced immunosuppression in the tumor microenvironment of most tumors (54, 55). The combination of an immune checkpoint inhibitor with one or more cytotoxic drug appears to be the most efficacious approach (56, 57) . Presumably, as cancer cells are killed by the cytotoxic chemotherapy, they trigger activation of antigen presenting cells that synergize with immune checkpoint inhibitors to produce a robust antitumor adaptive immune response. However, combination chemo-immunotherapy is associated with significantly more toxicities and many cancer patients are unfit and unable to tolerate the addition of chemotherapy due to poor performance status and comorbidities (58). In this respect, we believe that PLAD has a major potential in chemo-immunotherapy applications. Doxorubicin is a strong immunogenic cell death inducer and as such has intrinsic abscopal effects suggesting it can synergize with immune checkpoint blockade (59). Furthermore, its encapsulation in liposomes has been shown to significantly reduce drug toxicities in cancer patients. Recently, we showed that alendronate, when encapsulated in liposomes of similar composition to that of PLD, polarized macrophages towards an antitumoral M1-like phenotype and preferentially accumulated in tumor-draining lymph nodes and spleen (60) which are the primary sites for naïve T-cell priming and activation against tumor-associated antigens by antigen presenting cells such as macrophages. Our studies with PLAD showed increased uptake in spleen and tumor compared to PLD (18). Importantly, we found that PLAD shifted cellular drug uptake to TAM and to monocytic myeloid-derived suppressor cells (MDSC) and induced significant changes in number and functionality of tumor-infiltrating cells including TAM, MDSC, Treg, natural killer (NK), and NK-T cells (18) that are consistent with enhanced antitumor immune responses in the tumor microenvironment. We believe that the potent tumoricidal and immune stimulatory effects of PLAD makes it superior to PLD or conventional doxorubicin in chemo-immunotherapy regimens.

5. Conclusions

Co-encapsulation of ALD and DOX in pegylated liposomes leads to a chemo-immunotherapeutic, multi-modality platform with non-overlapping toxicity and with a unique mechanism of activity that may have a profound impact in cancer therapy. These results open the way for further development of PLAD towards clinical applications of a unique product that blends chemotherapeutic and immunomodulating properties.

Supplementary Materials: The following are available online at www.mdpi.com/xxx/s1, Figure S1: *In vitro* growth curve of Wehi-164 mouse sarcoma cells exposed for 72 h to free Dox, PLD or PLAD; Figure S2: Antitumor activity of PLAD combined with Vγ9Vδ2 T cells.

Author Contributions: "Conceptualization, AG, JM, NMLB; methodology, AG, HS, BD, APP, ACM, RTMR; validation and formal analysis, AG, HS, RTMR; investigation, AG, HS, BD, APP, JM, ACM, RTMR; resources, AG, JM, ; data curation, AG; writing—original draft preparation, AG; writing—review and editing, AG, HS, RTMR, NMLB; supervision, AG, HS, APP, RTMR; project administration, AG, HS, RTMR; funding acquisition, AG, JM, RTMR, NMLB. All authors have read and agreed to the published version of the manuscript."

Funding: "This research was funded in part by an unrestricted grant from Levco Pharmaceuticals Ltd. (Jerusalem, Israel). The imaging experiments were funded by the MITHRAS EPSRC programme [EP/S032789/1] and the Wellcome Trust EPSRC Centre for Medical Engineering at KCL [WT 203148/Z/16/Z], and by a Multi-User Equipment Grant [212885/Z/18/Z]. Further support for these studies comes from a Medical Research Council Confidence in Concepts award, the Experimental Cancer Medicine Centre at King's College London and by the National Institute for Health Research (NIHR) Biomedical Research Centre based at Guy's and St Thomas' NHS Foundation Trust and King's College London (grant number IS-BRC-1215-20006). N.M. La-Beck is supported by a grant from the National Institutes of Health (CA282339). The views expressed are those of the authors and not necessarily those of the NHS, the NIHR or the Department of Health.

Data Availability Statement: Data supporting reported results is available through the corresponding author.

Acknowledgments: The authors would like to thank Dr. Konstantin Adamsky (formerly from Levco Pharmaceuticals) for his great help in the organization of this research project, and Ms. Jenny Gorin, Lidia Mak, and Dina Tzemach for technical assistance with the experiments presented.

Conflicts of Interest: AG, HS, APP, and JM are co-inventors of the patent protecting the PLAD formulation. AG is medical consultant of Nextar Chempharma Ltd., a company providing CDMO services where PLAD was manufactured. JM is chief scientific officer of Leucid Bio, a company which has an interest in the development of CAR-engineered gamma delta T-cells. All other authors declare no conflict of interest. The company funding this study, Levco Pharmaceuticals, has been dissolved and the license of the patent protecting the PLAD product has been returned to Shaare Zedek Medical Center, the Hebrew University of Jerusalem, and Kings College London.

References

1. Franco MS, Oliveira MC. Liposomes Co- encapsulating Anticancer Drugs in Synergistic Ratios as an Approach to Promote Increased Efficacy and Greater Safety. Anticancer Agents Med Chem. 2019;19(1):17-28.
2. Tolcher AW, Mayer LD. Improving combination cancer therapy: the CombiPlex((R)) development platform. Future Oncol. 2018;14(13):1317-1332.
3. Zununi Vahed S, Salehi R, Davaran S, Sharifi S. Liposome-based drug co-delivery systems in cancer cells. Materials science & engineering C, Materials for biological applications. 2017;71:1327-1341.
4. Dicko A, Mayer LD, Tardi PG. Use of nanoscale delivery systems to maintain synergistic drug ratios in vivo. Expert Opin Drug Deliv. 2010;7(12):1329-1341.
5. Liboiron BD, Mayer LD. Nanoscale particulate systems for multidrug delivery: towards improved combination chemotherapy. Therapeutic delivery. 2014;5(2):149-171.
6. Duarte JA, Gomes ER, De Barros ALB, Leite EA. Co-Encapsulation of Simvastatin and Doxorubicin into pH-Sensitive Liposomes Enhances Antitumoral Activity in Breast Cancer Cell Lines. Pharmaceutics. 2023;15(2):369.
7. Ghaferi M, Raza A, Koohi M, Zahra W, Akbarzadeh A, Ebrahimi Shahmabadi H, Alavi SE. Impact of PEGylated Liposomal Doxorubicin and Carboplatin Combination on Glioblastoma. Pharmaceutics. 2022;14(10):2183.
8. Prasad P, Shuhendler A, Cai P, Rauth AM, Wu XY. Doxorubicin and mitomycin C co-loaded polymer-lipid hybrid nanoparticles inhibit growth of sensitive and multidrug resistant human mammary tumor xenografts. Cancer Lett. 2013;334(2):263-273.
9. Gabizon A, Ohana P, Amitay Y, Gorin J, Tzemach D, Mak L, Shmeeda H. Liposome co-encapsulation of anti-cancer agents for pharmacological optimization of nanomedicine-based combination chemotherapy. Cancer Drug Resist. 2021;4(2):463-484.
10. Mei KC, Liao YP, Jiang J, Chiang M, Khazaieli M, Liu X, Wang X, Liu Q, Chang CH, Zhang X, Li J, Ji Y, Melano B, Telesca D, Xia T, Meng H, Nel AE. Liposomal Delivery of Mitoxantrone and a Cholesteryl Indoximod Prodrug Provides Effective Chemo-immunotherapy in Multiple Solid Tumors. ACS Nano. 2020;14(10):13343-13366.
11. Mayer LD, Tardi P, Louie AC. CPX-351: a nanoscale liposomal co-formulation of daunorubicin and cytarabine with unique biodistribution and tumor cell uptake properties. Int J Nanomedicine. 2019;14:3819-3830.
12. Shmeeda H, Amitay Y, Gorin J, Tzemach D, Mak L, Stern ST, Barenholz Y, Gabizon A. Coencapsulation of alendronate and doxorubicin in pegylated liposomes: a novel formulation for chemoimmunotherapy of cancer. J Drug Target. 2016;24(9):878-889.
13. Gabizon AA, Patil Y, La-Beck NM. New insights and evolving role of pegylated liposomal doxorubicin in cancer therapy. Drug Resist Updat. 2016;29:90-106.
14. Clezardin P, Ebetino FH, Fournier PG. Bisphosphonates and cancer-induced bone disease: beyond their antiresorptive activity. Cancer research. 2005;65(12):4971-4974.
15. Teixeira S, Branco L, Fernandes MH, Costa-Rodrigues J. Bisphosphonates and Cancer: A Relationship Beyond the Antiresorptive Effects. Mini Rev Med Chem. 2019;19(12):988-998.
16. La-Beck NM, Liu X, Shmeeda H, Shudde C, Gabizon AA. Repurposing amino-bisphosphonates by liposome formulation for a new role in cancer treatment. Semin Cancer Biol. 2021;68:175-185.
17. Hodgins NO, Wang JT, Al-Jamal KT. Nano-technology based carriers for nitrogen-containing bisphosphonates delivery as sensitisers of γδ T cells for anticancer immunotherapy. Adv Drug Deliv Rev. 2017;114:143-160.
18. Islam MR, Patel J, Back PI, Shmeeda H, Adamsky K, Yang H, Alvarez C, Gabizon AA, La-Beck NM. Comparative effects of free doxorubicin, liposome encapsulated doxorubicin and liposome co-encapsulated

alendronate and doxorubicin (PLAD) on the tumor immunologic milieu in a mouse fibrosarcoma model. Nanotheranostics. 2022;6(4):451-464.

19. Patil Y, Shmeeda H, Amitay Y, Ohana P, Kumar S, Gabizon A. Targeting of folate-conjugated liposomes with co-entrapped drugs to prostate cancer cells via prostate-specific membrane antigen (PSMA). Nanomedicine. 2018;14(4):1407-1416.
20. Gabizon A, Horowitz AT, Goren D, Tzemach D, Shmeeda H, Zalipsky S. In vivo fate of folate-targeted polyethylene-glycol liposomes in tumor-bearing mice. Clin Cancer Res. 2003;9(17):6551-6559.
21. Edmonds S, Volpe A, Shmeeda H, Parente-Pereira AC, Radia R, Baguna-Torres J, Szanda I, Severin GW, Livieratos L, Blower PJ, Maher J, Fruhwirth GO, Gabizon A, de Rosales RTM. Exploiting the Metal-Chelating Properties of the Drug Cargo for In Vivo Positron Emission Tomography Imaging of Liposomal Nanomedicines. Acs Nano. 2016;10(11):10294-10307.
22. Thakur ML, Welch MJ, Joist JH, Coleman RE. In-111 Labeled Platelets - Studies on Preparation and Evaluation of in Vitro and in Vivo Functions. Thromb Res. 1976;9(4):345-357.
23. Parente-Pereira AC, Shmeeda H, Whilding LM, Zambirinis CP, Foster J, van der Stegen SJ, Beatson R, Zabinski T, Brewig N, Sosabowski JK, Mather S, Ghaem-Maghami S, Gabizon A, Maher J. Adoptive immunotherapy of epithelial ovarian cancer with Vgamma9Vdelta2 T cells, potentiated by liposomal alendronic acid. J Immunol. 2014;193(11):5557-5566.
24. Zhang S, Gao H, Bao G. Physical Principles of Nanoparticle Cellular Endocytosis. ACS Nano. 2015;9(9):8655-8671.
25. Gabizon A, Tzemach D, Gorin J, Mak L, Amitay Y, Shmeeda H, Zalipsky S. Improved therapeutic activity of folate-targeted liposomal doxorubicin in folate receptor-expressing tumor models. Cancer Chemother Pharmacol. 2010;66(1):43-52.
26. Horowitz AT, Barenholz Y, Gabizon AA. In vitro cytotoxicity of liposome-encapsulated doxorubicin: dependence on liposome composition and drug release. Biochim Biophys Acta. 1992;1109(2):203-209.
27. Shmeeda H, Amitay Y, Gorin J, Tzemach D, Mak L, Ogorka J, Kumar S, Zhang JA, Gabizon A. Delivery of zoledronic acid encapsulated in folate-targeted liposome results in potent in vitro cytotoxic activity on tumor cells. J Control Release. 2010;146(1):76-83.
28. Keller RK, Fliesler SJ. Mechanism of aminobisphosphonate action: characterization of alendronate inhibition of the isoprenoid pathway. Biochem Biophys Res Commun. 1999;266(2):560-563.
29. Kopecka J, Porto S, Lusa S, Gazzano E, Salzano G, Pinzòn-Daza ML, Giordano A, Desiderio V, Ghigo D, De Rosa G, Caraglia M, Riganti C. Zoledronic acid-encapsulating self-assembling nanoparticles and doxorubicin: a combinatorial approach to overcome simultaneously chemoresistance and immunoresistance in breast tumors. Oncotarget. 2016;7(15):20753-20772.
30. Gabizon AA, de Rosales RTM, La-Beck NM. Translational considerations in nanomedicine: The oncology perspective. Adv Drug Deliv Rev. 2020;158:140-157.
31. Harrington KJ, Rowlinson-Busza G, Syrigos KN, Abra RM, Uster PS, Peters AM, Stewart JS. Influence of tumour size on uptake of(111)ln-DTPA-labelled pegylated liposomes in a human tumour xenograft model. Br J Cancer. 2000;83(5):684-688.
32. Goren D, Horowitz AT, Tzemach D, Tarshish M, Zalipsky S, Gabizon A. Nuclear delivery of doxorubicin via folate-targeted liposomes with bypass of multidrug-resistance efflux pump. Clin Cancer Res. 2000;6(5):1949-1957.

33. Man F, Lim L, Volpe A, Gabizon A, Shmeeda H, Draper B, Parente-Pereira AC, Maher J, Blower PJ, Fruhwirth GO, R TMdR. In Vivo PET Tracking of (89)Zr-Labeled Vgamma9Vdelta2 T Cells to Mouse Xenograft Breast Tumors Activated with Liposomal Alendronate. Mol Ther. 2019;27(1):219-229.
34. Alfayez M, Kantarjian H, Kadia T, Ravandi-Kashani F, Daver N. CPX-351 (vyxeos) in AML. Leukemia & lymphoma. 2020;61(2):288-297.
35. Feldman EJ, Lancet JE, Kolitz JE, Ritchie EK, Roboz GJ, List AF, Allen SL, Asatiani E, Mayer LD, Swenson C, Louie AC. First-in-man study of CPX-351: a liposomal carrier containing cytarabine and daunorubicin in a fixed 5:1 molar ratio for the treatment of relapsed and refractory acute myeloid leukemia. J Clin Oncol. 2011;29(8):979-985.
36. Batist G, Gelmon KA, Chi KN, Miller WH, Jr., Chia SK, Mayer LD, Swenson CE, Janoff AS, Louie AC. Safety, pharmacokinetics, and efficacy of CPX-1 liposome injection in patients with advanced solid tumors. Clinical cancer research : an official journal of the American Association for Cancer Research. 2009;15(2):692-700.
37. Tardi PG, Dos Santos N, Harasym TO, Johnstone SA, Zisman N, Tsang AW, Bermudes DG, Mayer LD. Drug ratio-dependent antitumor activity of irinotecan and cisplatin combinations in vitro and in vivo. Mol Cancer Ther. 2009;8(8):2266-2275.
38. Zhang RX, Cai P, Zhang T, Chen K, Li J, Cheng J, Pang KS, Adissu HA, Rauth AM, Wu XY. Polymer-lipid hybrid nanoparticles synchronize pharmacokinetics of co-encapsulated doxorubicin-mitomycin C and enable their spatiotemporal co-delivery and local bioavailability in breast tumor. Nanomedicine : nanotechnology, biology, and medicine. 2016;12(5):1279-1290.
39. Sprooten J, Laureano RS, Vanmeerbeek I, Govaerts J, Naulaerts S, Borras DM, Kinget L, Fucikova J, Spisek R, Jelinkova LP, Kepp O, Kroemer G, Krysko DV, Coosemans A, Vaes RDW, De Ruysscher D, De Vleeschouwer S, Wauters E, Smits E, Tejpar S, Beuselinck B, Hatse S, Wildiers H, Clement PM, Vandenabeele P, Zitvogel L, Garg AD. Trial watch: chemotherapy-induced immunogenic cell death in oncology. Oncoimmunology. 2023;12(1):2219591.
40. La-Beck NM, Gabizon AA. Nanoparticle Interactions with the Immune System: Clinical Implications for Liposome-Based Cancer Chemotherapy. Front Immunol. 2017;8:416.
41. Mantovani A, Allavena P, Marchesi F, Garlanda C. Macrophages as tools and targets in cancer therapy. Nat Rev Drug Discov. 2022;21(11):799-820.
42. Gabizon A, Cherny N, Isacson R, AbuRemilah A, Shmeeda H, Rosengarten O. A phase 1b study of chemoimmunotherapy with pegylated liposomal Doxorubicin and pembrolizumab in estrogen receptor-positive, endocrine-resistant breast cancer. Journal of Clinical Oncology. 2021;39(15):1049-1049.
43. Lee EK, Xiong N, Cheng SC, Barry WT, Penson RT, Konstantinopoulos PA, Hoffman MA, Horowitz N, Dizon DS, Stover EH, Wright AA, Campos SM, Krasner C, Morrissey S, Whalen C, Quinn R, Matulonis UA, Liu JF. Combined pembrolizumab and pegylated liposomal doxorubicin in platinum resistant ovarian cancer: A phase 2 clinical trial. Gynecologic oncology. 2020;159(1):72-78.
44. Rossevold AH, Andresen NK, Bjerre CA, Gilje B, Jakobsen EH, Raj SX, Falk RS, Russnes HG, Jahr T, Mathiesen RR, Lomo J, Garred O, Chauhan SK, Lereim RR, Dunn C, Naume B, Kyte JA. Atezolizumab plus anthracycline-based chemotherapy in metastatic triple-negative breast cancer: the randomized, double-blind phase 2b ALICE trial. Nat Med. 2022;28(12):2573-2583.
45. Kyte JA, Andresen NK, Russnes HG, Fretland SO, Falk RS, Lingjaerde OC, Naume B. ICON: a randomized phase IIb study evaluating immunogenic chemotherapy combined with ipilimumab and nivolumab in patients with metastatic hormone receptor positive breast cancer. J Transl Med. 2020;18(1):269.

46. Edmonds S, Volpe A, Shmeeda H, Parente-Pereira AC, Radia R, Baguna-Torres J, Szanda I, Severin GW, Livieratos L, Blower PJ, Maher J, Fruhwirth GO, Gabizon A, R TMdR. Exploiting the Metal-Chelating Properties of the Drug Cargo for In Vivo Positron Emission Tomography Imaging of Liposomal Nanomedicines. ACS Nano. 2016;10(11):10294-10307.
47. Man F, Lammers T, R TMdR. Imaging Nanomedicine-Based Drug Delivery: a Review of Clinical Studies. Mol Imaging Biol. 2018;20(5):683-695.
48. Prabhakar U, Maeda H, Jain RK, Sevick-Muraca EM, Zamboni W, Farokhzad OC, Barry ST, Gabizon A, Grodzinski P, Blakey DC. Challenges and key considerations of the enhanced permeability and retention effect for nanomedicine drug delivery in oncology. Cancer Res. 2013;73(8):2412-2417.
49. Golombek SK, May JN, Theek B, Appold L, Drude N, Kiessling F, Lammers T. Tumor targeting via EPR: Strategies to enhance patient responses. Adv Drug Deliv Rev. 2018;130:17-38.
50. Kim J, Cho H, Lim DK, Joo MK, Kim K. Perspectives for Improving the Tumor Targeting of Nanomedicine via the EPR Effect in Clinical Tumors. Int J Mol Sci. 2023;24(12).
51. Rajan R, Sabnani MK, Mavinkurve V, Shmeeda H, Mansouri H, Bonkoungou S, Le AD, Wood LM, Gabizon AA, La-Beck NM. Liposome-induced immunosuppression and tumor growth is mediated by macrophages and mitigated by liposome-encapsulated alendronate. J Control Release. 2018;271:139-148.
52. La-Beck NM, Nguyen DT, Le AD, Alzghari SK, Trinh ST. Optimizing Patient Outcomes with PD-1/PD-L1 Immune Checkpoint Inhibitors for the First-Line Treatment of Advanced Non-Small Cell Lung Cancer. Pharmacotherapy. 2020;40(3):239-255.
53. Robert C. A decade of immune-checkpoint inhibitors in cancer therapy. Nature Communications. 2020;11(1):3801.
54. Peranzoni E, Lemoine J, Vimeux L, Feuillet V, Barrin S, Kantari-Mimoun C, Bercovici N, Guerin M, Biton J, Ouakrim H, Regnier F, Lupo A, Alifano M, Damotte D, Donnadieu E. Macrophages impede CD8 T cells from reaching tumor cells and limit the efficacy of anti-PD-1 treatment. Proc Natl Acad Sci U S A. 2018;115(17):E4041-E4050.
55. Sharma P, Hu-Lieskovan S, Wargo JA, Ribas A. Primary, Adaptive, and Acquired Resistance to Cancer Immunotherapy. Cell. 2017;168(4):707-723.
56. La-Beck NM, Jean GW, Huynh C, Alzghari SK, Lowe DB. Immune Checkpoint Inhibitors: New Insights and Current Place in Cancer Therapy. Pharmacotherapy. 2015;35(10):963-976.
57. Ghiringhelli F, Rébé C. Using immunogenic cell death to improve anticancer efficacy of immune checkpoint inhibitors: From basic science to clinical application. Immunol Rev. 2023.
58. Trinh S, Le A, Gowani S, La-Beck NM. Management of Immune-Related Adverse Events Associated with Immune Checkpoint Inhibitor Therapy: a Minireview of Current Clinical Guidelines. Asia Pac J Oncol Nurs. 2019;6(2):154-160.
59. Shi F, Huang X, Hong Z, Lu N, Huang X, Liu L, Liang T, Bai X. Improvement strategy for immune checkpoint blockade: A focus on the combination with immunogenic cell death inducers. Cancer Lett. 2023;562:216167.
60. Islam MR, Patel J, Back PI, Shmeeda H, Kallem RR, Shudde C, Markiewski M, Putnam WC, Gabizon AA, La-Beck NM. Pegylated Liposomal Alendronate Biodistribution, Immune Modulation, and Tumor Growth Inhibition in a Murine Melanoma Model. Biomolecules. 2023;13(9):1309.